

A computationally efficient method for the limit elasto plastic analysis of space frames

M. Papadrakakis, V. Papadopoulos

132

Abstract A computationally efficient method for the first order step-by-step limit analysis of space frames is presented. The incremental non-holonomic analysis is based on the generalized plastic node method. The non-linear yield surface is approximated by a multi-faceted surface, thus avoiding the iterative formulation at each load step. In order to prevent the occurrence of very small load steps a second internal and homothetic to the initial yield surface is implemented which creates a plastic zone for the activation of the plastic modes. This implementation reduces substantially the computational effort of the procedure without affecting the value of the final load. The solution of the linear equilibrium equation at each load step is obtained with the preconditioned conjugate gradient method. Special attention is paid to the fact that the overall stiffness matrix changes gradually with the successive formation of plastic nodes. The application of the conjugate gradient method is based on some recent developments on improved matrix handling techniques and efficient preconditioning strategies. A number of test problems have been performed which show the usefulness of the proposed approach and its superiority in respect to efficient direct methods of solution in both storage requirements and computing time.

1

Introduction

The load carrying capacity of space frames has been the subject of extensive research over the last five to ten years. This is because the behaviour of these structures is significantly affected by the progressive development of plastic zones at critical section on account of material and geometric non-linearities. In contrast to the investigation of the limit state response of plane frames, where both mathematical programming and step by step approaches have been implemented, in three-dimensional building frames the incremental step by step approach has been mainly used. The use of incremental variational principles together with the finite element method has made it possible to develop finite element models and computational algorithms that can handle all types of nonlinearities to any desired degree of accuracy. Although the plastic hinge or concentrated plasticity approach provides only an approximate representation of the member behaviour,

as opposed to the plastic zone or distributed plasticity approach, it is considerably more cost effective. In this context a number of papers have recently appeared, based on the plastic hinge model for treating materially non-linear space frame problems and incorporating second order step-by-step analyses using an incremental iterative formulation (Ueda and Yao 1982; Orbison et al. 1982; Argyris et al. 1982; Hilmy and Abel 1985; Powell and Chen 1986; Bozzo and Gambarotta 1985; Kondoh and Atluri 1987; Shi and Atluri 1988; Shi and Atluri 1989; Shi and Atluri 1992; Tin-Loi and Wong 1989; Conci and Gattass 1990; Bermiani and Kitpornchai 1990; Kiny et al. 1993; Ziemian et al. 1993; Izzudin and Elnashai 1993).

As opposed to the disadvantages of mathematical programming approaches which are based on rigid plastic analysis, purely incremental elasto-plastic analyses provide the complete load-deflection curve giving information on the structural behaviour prior to collapse and the deflections at collapse, while reversible loading paths and geometrical non-linearities can also be taken into account. The incremental elasto-plastic analyses based on multi-faceted yield surfaces and using elementary matrix structural analysis concepts provide a compact and practical approach for modelling the inelastic global structural behaviour of steel beam-column use of non-linear algorithms for the solution of the governing non-linear equations and may result to significant computational advantages. They can also provide very realistic results in a great variety of moment resisting frames as the over prediction of stiffness and strength becomes significant only for slender frames with intensive vertical loading (Argyris et al. 1982; Morris 1990). Therefore, it is very helpful for the design engineer to use an efficient and cost-effective approach to treat large realistic 3-D building frames, which will give the opportunity to test a number of design options leading to a more optimal design. Subsequently the analysis may be supplemented by a more refined incremental-iterative procedure.

In this work the incremental non-holonomic analysis is based on the generalised plastic node concept as described by Ueda et al. (1982) and Orbison et al. (1982). The non-linear yield surface is approximated by a multi-faceted surface, thus avoiding the iterative formulation at each load step which is necessary for the simultaneous fulfilment of yield and equilibrium conditions. Much emphasis is given to the solution procedure of the governing equilibrium equations as the load increases until the final collapse value is attained. The solution of the linear equilibrium equations at each load step is obtained using the preconditioned conjugate gradient method. The handling of the preconditioning matrix takes into account the fact that the overall stiffness matrix changes gradually with the successive formation of the plastic nodes. Thus, the

Communicated by D. Beskos, 24 January 1995

M. Papadrakakis, V. Papadopoulos
Institute of Structural Analysis and Aseismic Research, National
Technical University of Athens, Athens 15773, Greece

Correspondence to: M. Papadrakakis

preconditioning matrix need not be formed at every step but only when a substantial deterioration of the stiffness matrix is realised, due to the successive formation of the plastic nodes.

This paper is an extension of previous work by Papadrakakis and Karamanos (1991) where plane frame studies were presented. The novelty of the present work in relation to the previous one is, apart from the formulation of the problem in three dimensions, the computational handling of the yield criterion and the implementation of some recent developments in the equation solving procedure which further enhance the efficiency of the proposed technique. In order to prevent the occurrence of very small load steps, associated with multi-faceted yield surfaces and avoid spurious oscillations of a yield point around sharp corners, a yield zone concept is adopted by introducing a second internal yield surface, homothetic and close to the first one. This handling of the yield criterion substantially increases the size of the load steps without impairing the accuracy of the solution. The implementation of some recent developments of the conjugate gradient method particularly suitable for three dimensional applications in respect to improved matrix handling techniques and efficient preconditioning strategies, as proposed by Papadrakakis (1993) and Papadrakakis and Bitoulas (1991, 1993) result in even more cost effective solution both in terms of computing time and storage requirements. The numerical results presented demonstrate that this approach provides a realistic treatment for the analysis of 3-D building frames of substantial size.

2 The plastic node method

2.1 The elasto-plastic stiffness matrix

Under the assumption of concentrated plasticity all plastic deformations are confined to zero length plastic zones at the two ends of the member, leaving elastic the part of the member between the two plastic nodes. The materials are assumed to be elastic-perfectly plastic and the structural response is in the range of small displacements. According to this theory when the stress resultants satisfy a prescribed yielding function at the ends of the element, a plastic node will occur instantly at that location. After reaching the yield surface, and in the absence of strain hardening, the stress point moves on the yield surface provided that stress reversals have not occurred. This approach was introduced by Ueda and Yao (1982) and is referred to as the plastic node method.

Assuming that for the 3-D beam element of Fig. 1 there is interaction between axial and biaxial bending effects, the plasticity conditions at the two element nodes may be stated as follows:

$$F_1 = F_1(S_1, S_5, S_6, \sigma_y) \quad \text{for member end} \quad (1)$$

$$F_2 = F_2(S_7, S_{11}, S_{12}, \sigma_y) \quad \text{for member end2} \quad (2)$$

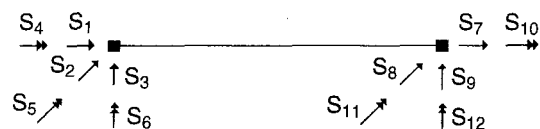


Fig. 1. Element nodal forces

where S_1, S_7 are the axial and S_5, S_6, S_{11}, S_{12} are the bending stress resultants respectively and σ_y is the yield stress. If $F_j < 0$ the behaviour is elastic, while $F_j = 0$ corresponds to the formation of a plastic hinge at the end j . The tangent elasto-plastic stiffness may be expressed as:

$$K_{ep} = K_e - K_e \Phi \{ \Phi^T K_e \Phi \}^{-1} \Phi^T K_e \quad (3)$$

in which K_{ep} is the elasto-plastic element stiffness matrix, K_e is the elastic element stiffness matrix, and Φ is defined as follows:

$$\Phi = \Phi_1 = \left[\frac{\partial F}{\partial S_1} \ 0 \ 0 \ 0 \ \frac{\partial F}{\partial S_5} \ \frac{\partial F}{\partial S_6} \ 0 \ 0 \ 0 \ 0 \ 0 \ 0 \right]^T \quad (4)$$

$$\Phi = \Phi_2 = \left[0 \ 0 \ 0 \ 0 \ 0 \ 0 \ \frac{\partial F}{\partial S_7} \ 0 \ 0 \ 0 \ \frac{\partial F}{\partial S_{11}} \ \frac{\partial F}{\partial S_{12}} \right]^T \quad (5)$$

or

$$\Phi = [\Phi_1 \ \Phi_2]^T \quad (6)$$

if plastic nodes are formed at the ends 1,2 or 1 and 2, respectively.

Stress reversals can be detected by monitoring the sign of the scalar $d\mu_j$ which defines the increment of the plastic nodal displacement in the associated plasticity conditions

$$d\mathbf{u}_p = d\mu_j \Phi_j \quad \text{for } j = 1, 2 \quad (7)$$

in which the two-component vector $d\mathbf{u}$ is given by

$$d\mathbf{u} = (\Phi^T K_e \Phi)^{-1} \Phi^T K_e d\mathbf{u} \quad (8)$$

Thus, when the plastic hinge is under loading, $d\mu_j$ is positive; otherwise when unloading occurs $d\mu_j$ becomes negative.

2.2 Yield criteria

For the purpose of the limit state analysis using the above mentioned formulation, a plastic interaction surface in terms of stress resultants has to be derived. The known yield conditions in terms of stress components must therefore be transformed to the space of the generalized forces. The existence of a large number of different limit state conditions are reflected in the variety of the interaction surfaces used. In general, the yield surface can be represented by a single equation or a multi-faceted surface. Closed form interactive expressions are however limited in the literature to special cases corresponding to the dominant behaviour of the structural components instead of coping with general cases which involve all six generalised cross-sectional forces. These closed form expressions, which appear in a single equation, are strongly dependent on the cross-sectional geometric properties. For the analysis of a 3-D space frame, a simplified limit state condition would only require the selection of the axial force and the two bending moments as sufficient parameters to describe the interaction surfaces.

Following these lines, the equation proposed by Orbison et al. (1982) was selected. This is given in a single equation by the

expression:

$$1.15p^2 + m_z^4 + m_y^4 + 3.67p^2m_z^2 + 3p^6m_y^2 + 4.65m_z^4m_y^2 = 1 \quad (9)$$

where p , m_z , m_y identify P/P_y , M_z/M_{pz} , P_y/M_{py} , respectively. P_y is the squash load, while M_{pz} and M_{py} are the plastic moment of the strong and weak axis. This equation is only representative for light to medium weight American shapes and provides an excellent correlation with the surfaces derived for a W12 × 31 section and with recommendation of codes (Conci and Gattass 1990).

Further on, supporting the simplicity of our approach in terms of the required mathematical formulation, two piece-wise linear multi-faceted surfaces which approximate the above equation were used as shown in Fig. 2. The approach is general, however, and any other surface can easily be implemented by simply changing the equations of the consisting hyperplanes.

Although the single equation surface has potential advantages over the multi-faceted surface, as pointed out by Orbison et al. (1982), an iterative procedure is typically required to determine the load increment from an elastic state to incipient yielding. However, when planar facets are used, the gradient vector Φ contains constant terms only and is therefore independent of the current forces. Thus, K_{ep} remains constant within the load increment and the elasto-plastic equilibrium states are obtained using a pure incremental procedure without iterations. This transformation of the non-linear problem into a linear one is necessary, at each load step in which satisfaction of both equilibrium and yield criteria is easily achieved, in order to implement the solution techniques described in the following section.

2.3

Computer implementation

The total applied load vector is given by

$$\mathbf{f} = \lambda \mathbf{q} \quad (10)$$

where \mathbf{q} is the basic load vector usually indicating the magnitude of the structure loads and the scalar λ is the load factor. As

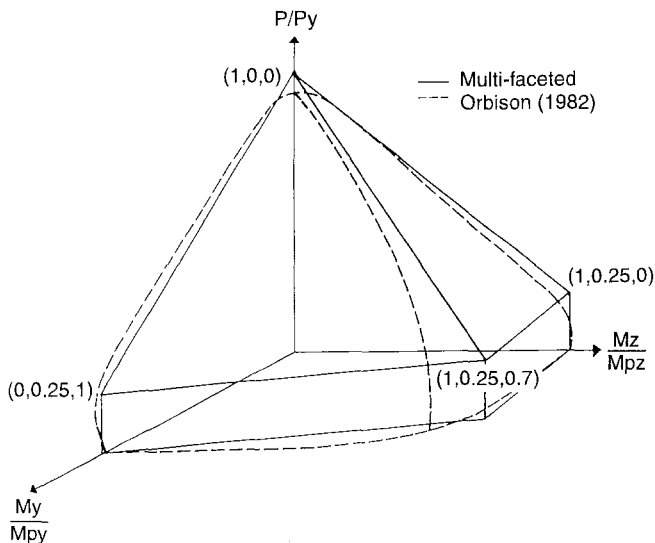
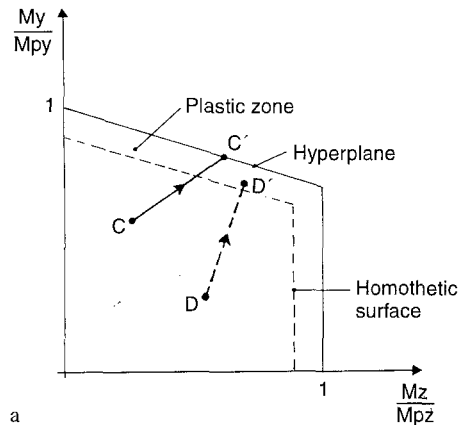


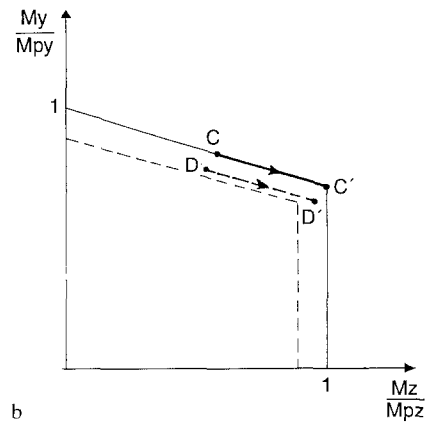
Fig. 2. Yield surface and multi-faceted approximation

λ increases, plastic nodes are formed until the structure collapses, after becoming a mechanism. The aim of the computational procedure is the evaluation of that ultimate load factor λ_u . This is done through a pure incremental procedure since the K_{ep} matrix is a constant tangential matrix within the load increment, which depends only on the co-ordinates of the normal vector Φ of the hyperplane at which the force point is found. When increasing the scalar λ a force point, corresponding to an end-section of an element, either moves from the elastic region inside the yield surface to a point on the yield surface or, if this point has already reached the yield surface at a previous step, from the point on a hyperplane to the intersection of this hyperplane with the neighbouring one (Fig. 3). This indicates the activation of a new yield mode and since the yield surface is piece-wise linear, the behaviour of the structure between two subsequent yield mode activations is also linear. Violations of the yield condition and equilibrium do not occur, as with analyses involving non-linear yield surfaces. An important feature of the analysis is the automatic calculation of the maximum load increment which corresponds to the activation of a new yield mode.

The usual problem occurring with multi-faceted surfaces when implemented to 3-D problems is that many steps are frequently required before the ultimate load is reached. This is not only because each plastic node formation requires a full analysis step, but also because a change of force point from one hyperplane to another would also require a full analysis step.



a



b

Fig. 3a, b. Estimation of load increment CC' and representation of plastic zone for further activation of yield modes DD' . a Yield activation from elastic state b Yield activation from adjacent hyperplane

Additionally, spurious oscillations of a point around sharp corners of the yield surface may occur due to the discontinuity of the derivative vector Φ (Orbison et al. 1982). For large-scale problems, these factors introduce significant numerical instabilities, to the point of sometimes rendering the approach incapable of reaching the true ultimate load. In order to avoid these implications, the use of a second internal yield surface of similar orientation (*homothetic*) and close to the first one is introduced by Bozzo and Gambarota (1983) for 2-D frames. The original yield surface together with its homothetic create a zone with well defined dimensions where the activation of a yield mode starts as soon as the force point of an element-end crosses the internal surface (CC' and DD' paths of Fig. 3a). This force point is then restricted to the interior of this zone, unless unloading occurs (CC' and DD' paths of Fig. 3b). This implementation allows the activation of more than one yield mode within the same load step. In our application the distance between the two yield surfaces is defined by a tolerance criterion ε_s which controls the activation of a yield mode. In this way we avoid the dependence of the development of the plastic nodes on the accuracy with which the yield criterion is satisfied. Thus, instead of a force point oscillating around a sharp corner for a number of steps without any advancement on the loading path, simultaneous formation of more than one plastic nodes will change significantly the global stiffness characteristics forcing the oscillating point to move towards a new direction away from the corner of oscillation. This has repetitively been observed in our examples. The introduction of the homothetic surface in our implementation reduces substantially the computational time of the procedure without affecting the accuracy of the solution. The influence of the tolerance ε_s on the accuracy and the efficiency of the solution is shown in Table 3 of the section Test Problems.

The automatic calculation of the load increment corresponding to the initiation of a new yield mode is performed by computing the shortest distance (CC' in Fig. 3) required for the activation of a new hyperplane from an elastic state or for the migration of a force point to an adjacent hyperplane. For each member-end the corresponding distance is calculated as follows. The incremental force vector \mathbf{A}_i for element i expressed in the yield surface space is given by

$$\mathbf{A}_i = [\mathbf{A}_1^T \mathbf{A}_2^T] = \left[\frac{dS_1}{P_y} \frac{dS_5}{M_{py}} \frac{dS_6}{M_{pz}} \frac{dS_7}{P_y} \frac{dS_{11}}{M_{py}} \frac{dS_{12}}{M_{pz}} \right]^T \quad (11)$$

The parametric equations for member-end 1 of the line which is parallel to the vector \mathbf{A}_1 and passes from the cumulative force state of the current load step (point C in Fig. 3), are expressed by

$$\begin{aligned} x &= \frac{S_1}{P_y} + \frac{dS_1}{P_y} Dt \\ y &= \frac{S_5}{M_{py}} + \frac{dS_5}{M_{py}} Dt \\ z &= \frac{S_6}{M_{pz}} + \frac{dS_6}{M_{pz}} Dt \end{aligned} \quad (12)$$

Similar expressions may be derived for member-end 2 by using the corresponding element forces. The general equation of

a plane of the multi-faceted yield surface is given by

$$\alpha x + \beta y + \gamma z + \delta = 0 \quad (13)$$

In order to calculate the distance, i.e. the scalar Dt_{ij} by which the vector \mathbf{A}_j must be multiplied in order to reach the plane defined by Eq. (13), the intersection point of the line of Eq. (12) and the plane of Eq. (13) must be defined. Thus the required distance is determined by substituting x, y, z of Eq. (12) into Eq. (13) and solving for Dt_{ij} . Then the load increment for the next step is obtained from

$$\delta\lambda = \min(Dt_{ij}) \quad (14)$$

The computational procedure may be described in the following stages:

1. Initial formulation using the elastic matrices of the elements. Step number $m = 1$.
2. Solve for the incremental basic displacements in step m : $d\mathbf{u}_m = \mathbf{K}_m^{-1} \mathbf{q}$, where \mathbf{K}_m is the overall stiffness matrix at step m . If diagonal terms resulting from the factorization of the stiffness matrix are negative or displacements are too large, then the structure has become a mechanism and the incremental procedure is terminated.
3. Evaluate the incremental forces, $d\mathbf{S}_i = [dS_1 \ dS_5 \ dS_6 \ dS_7 \ dS_{11} \ dS_{12}]^T$ due to $d\mathbf{u}_m$, for each element i .
4. Find the shortest distance between the force point of the element-ends and the yield surface, or the point on a hyperplane and the intersection with the neighbouring one according to Eq. (14).
5. Calculate $\delta_{ij} = Dt_{ij} - \delta\lambda$ for all elements. If $\delta_{ij} \leq \varepsilon_s$ ($\varepsilon_s = 0.01$) then end j of element i will become plastic.
6. Update load factor, displacements and element forces.

$$\lambda_m = \lambda_{m-1} + \delta\lambda_m \quad (15)$$

$$\mathbf{u}_m = \mathbf{u}_{m-1} + \delta\lambda_m \mathbf{u}_m \quad (16)$$

$$\mathbf{S}_m = \mathbf{S}_{m-1} + \delta\lambda_m d\mathbf{S} \quad \text{for each member} \quad (17)$$

7. Check for unloading according to Eq. (8).
8. The overall stiffness matrix is altered by the new stiffness matrix of the element(s) taking into consideration the newly formed plastic conditions. Some additional changes are required if stress reversals occur.
9. Set $m = m + 1$ and return to step 2.

3

Solution techniques

3.1

The preconditioned conjugate gradient method

The incremental limit analysis of space frames, described in the previous section, requires a number of subsequent linear solutions in which the overall stiffness matrix is slightly modified from one solution to the other. The total number of solutions corresponds to the total number of load increments required for the structure to become a mechanism. The change of stiffness from one step to the other is only due to the contribution of the elasto-plastic stiffness matrices of the

elements with the newly formed plastic nodes. These special features of the problem make the preconditioned conjugate gradient method (PCG) very attractive for the solution of the linear problem at each load increment. The PCG is established as the more attractive iterative procedure for solving linear problems resulting from the finite element discretization. An important factor in the success of this method in solving large-scale finite element equations is the preconditioned technique used to improve the ellipticity of the coefficient matrix. This typically consists of replacing the original system $\mathbf{Ku} = \mathbf{f}$ by the equivalent system

$$\mathbf{R}^{-1}\mathbf{Ku} = \mathbf{R}^{-1}\mathbf{f} \quad (18)$$

where \mathbf{K} is the $(n \times n)$ stiffness matrix and the transformation or preconditioning matrix \mathbf{R} is an approximation to \mathbf{K} and it is non-singular. The PCG algorithm, based on the most efficient conjugate gradient version in respect to computational labour, storage requirements and accuracy is defined as follows for the untransformed variables:

$$\begin{aligned} \alpha_m &= \frac{(\mathbf{r}^{(m)}, \mathbf{z}^{(m)})}{(\mathbf{d}^{(m)}, \mathbf{Kd}^{(m)})} \\ \mathbf{u}^{(m+1)} &= \mathbf{u}^{(m)} + \alpha_m \mathbf{d}^{(m)} \\ \mathbf{r}^{(m+1)} &= \mathbf{r}^{(m)} + \alpha_m \mathbf{Kd}^{(m)} \\ \text{if } \|\mathbf{r}^{(m+1)}\| / \|\mathbf{f}\| &\leq \varepsilon \text{ then stop} \\ \mathbf{z}^{(m+1)} &= \mathbf{R}^{-1}\mathbf{r}^{(m+1)} \\ \beta_m &= \frac{(\mathbf{r}^{(m+1)}, \mathbf{z}^{(m+1)})}{(\mathbf{r}^{(m)}, \mathbf{z}^{(m)})} \\ \mathbf{d}^{(m+1)} &= -\mathbf{z}^{(m+1)} + \beta_m \mathbf{d}^{(m)} \\ \text{with } \mathbf{r}^{(0)} &= \mathbf{Ku}^{(0)} - \mathbf{f}, \quad \mathbf{z}^{(0)} = \mathbf{R}^{-1}\mathbf{r}^{(0)}, \quad \mathbf{d}^{(0)} = \mathbf{z}^{(0)} \end{aligned} \quad (19)$$

At the heart of the PCG iterative procedure for solving $\mathbf{Ku} = \mathbf{f}$ is the determination of the residual vector and the selection of the preconditioning matrix. The accuracy achieved and the computational labour of the method is largely determined by how these two parameters are selected. An extensive study performed by Papadrakakis and Bitoulas (1993) revealed that the computation of the residual vector from its defining formula $\mathbf{r}^{(m)} = \mathbf{Ku}^{(m)} - \mathbf{f}$ with an explicit or a first order differences matrix-vector multiplication $\mathbf{Ku}^{(m)}$ offers no improvement in the accuracy of the computed results. In fact, it was found that, contrary to previous recommendations, the calculation of the residuals by the recursive expression of algorithm (19) produces a more stable and well-behaved iterative procedure. Based on this observation a mixed precision PCG implementation is proposed in which all computations are performed in single precision, except for double precision computation of the matrix vector multiplication in the recursive evaluation of the residual vector. This implementation is a robust and reliable solution procedure even for handling large and ill-conditioned problems, while it is also storage-effective. It was also proved

to be more cost effective, for the same storage demands, than double precision calculations.

3.2 Preconditioning matrices

A number of strategies can be used to increase the efficiency of linear iterative solvers based on the selection and implementation of the preconditioning matrix in conjunction with different ways of handling the matrix equations. The resulting hybrid direct-iterative procedure is more effective than the exclusive use of either a direct or a pure iterative approach (Papadrakakis 1993).

The preconditioning matrix \mathbf{R} has to be selected appropriately so that the eigenvalues of $\mathbf{R}^{-1}\mathbf{K}$ are spread over a much narrower range than those of \mathbf{K} . Preconditioning and matrix handling strategies may be classified into three main categories: global, element-by-element and block and domain decomposition. The two latter implementations are particularly suitable on innovative computer architectures with parallel processing capabilities. The most widely used global preconditioners are derived either from the incomplete Cholesky factorization of the stiffness matrix (ICPR) or from the symmetric successive overrelaxation (SSOR) characteristic matrix. The reason for performing an incomplete factorization is to obtain a reasonable factorization of \mathbf{K} without generating too many fill-ins. Such an approach leads to the factorization $\mathbf{LL}^T = \mathbf{K} - \mathbf{E}$, where \mathbf{E} is an error matrix which does not have to be formed. The SSOR implementation for \mathbf{R} is suitable for problems where available computing storage is liable to be stretched to its limit, since no additional storage is required for the preconditioning matrix \mathbf{R} . Ajiz and Jennings (1984) proposed a robust incomplete factorization-based preconditioner in which rejection of an off-diagonal term during factorization, takes place according to its magnitude relative to the diagonal terms corresponding to its row and column. If the off-diagonal term is rejected, the corresponding diagonal terms are modified in order to preserve the stability of the factorization process. The proposed computer implementation however, requires complicated addressings and high demands for auxiliary storage during the formation of the preconditioning matrix. In this study an improved computer implementation of this incomplete factorization type preconditioner is used. This version proposed by Bitoulas and Papadrakakis (1993) was found to be particularly effective in large-scale 3-D problems by reducing both the computing storage and the factorization time in respect to the original version.

The ICPR algorithm can be described using a row-by-row formulation and referring to \mathbf{L}^T rather than \mathbf{L} , as follows:

for each row $i = 1, 2, \dots, N$
for each column $j = i + 1, \dots, N$

$$k_{ij}^* = k_{ij} - \sum_{k=1}^{i-1} l_{ki} l_{kj}$$

$$\bar{k}_{ii} = k_{ii} + \sum_{k=1}^{i-1} c_{ii}^k + \sum_{k=i+1}^{j-1} c_{ii}^{(k)} - \sum_{k=1}^{i-1} l_{ki} l_{ki}$$

$$\bar{k}_{jj} = k_{jj} + \sum_{k=1}^{i-1} c_{jj}^{(k)}$$

$$\text{check for rejection: } k_{ij}^* < \psi \bar{k}_{ii} \bar{k}_{jj} \quad (20)$$

$$\text{if yes: } c_{ii}^{(j)} = (\bar{k}_{ii} / \bar{k}_{jj})^{1/2} |k_{ij}^*|$$

$$c_{jj}^{(i)} = (\bar{k}_{jj} / \bar{k}_{ii})^{1/2} |k_{ij}^*|$$

$$k_{ij}^* = 0$$

next j

$$l_{ii} = (\bar{k}_{ii})^{1/2}$$

for each column $j = i + 1, \dots, N$

$$l_{ij} = k_{ij}^* / l_{ii}$$

next j

next i

In the above description l_{ij} is the entry in the row and column j of L^T . The choice for $\psi = 0$ corresponds to the complete factorization while in the case of $\psi = 1$ corresponds to a form of diagonal scaling.

The second type of preconditioning used in this study corresponds to the SSOR characteristic matrix and is defined as

$$\mathbf{R} = (\mathbf{D} + \omega\mathbf{C})\mathbf{D}^{-1}(\mathbf{D} + \omega\mathbf{C}^T) \quad (21)$$

where $\mathbf{K} = \mathbf{D} + \mathbf{C} + \mathbf{C}^T$, \mathbf{D} is diagonal and \mathbf{C} is strictly lower triangular. When $\omega = 0$ the preconditioning matrix reduces to diagonal. The advantage of this type of preconditioner is that no extra storage is required for \mathbf{R} , since it can be easily formed from \mathbf{K} .

3.3 The complete Cholesky LDL^T factorization

In this study the proposed solution technique is compared to a conventional direct method for the solution of the linear equations at each load step. One of the most efficient direct solution is considered to be the LDL^T Cholesky factorization of the stiffness matrix stored in skyline form (Bathe and Wilson 1976). Since for large-scale 3-D frames the solution phase at each load step represents a significant investment in computing effort, a simple modification in the factorized process is implemented resulting in significant savings in computing time. During the factorization phase the alterations to the factorized stiffness matrix are confined to the bottom right-hand corner starting from the first node with a change in the stiffness matrix due to the plastic node formation at the end of one or more elements connected to that node. Consequently the time-consuming factorization part need not be repeated but only the steps after the smallest degree of freedom which is affected by the change of stiffness matrix and onwards. In this implementation, however, the stiffness matrix is not replaced by the factorized matrix \mathbf{L} as in ordinary linear problems, but has to be stored separately, incorporating the changes due to the plastic node formation, so that the factorization can be restored at the appropriate point at the next load step. This technique is referred to as a modified complete factorization.

4

Test problems

Three test examples have been carried out in order to test the performance of the methods previously described. Two yield surfaces (a) and (b), shown in Fig. 5 in the plane $m_y - m_z$, are used for the analysis of example 1, to investigate the sensitivity of the results on different approximations of the yield surface represented by Eq. (9). Yield surface (a) is used for the subsequent examples 2 and 3. A compact storage scheme is used for PCG-ICPR to store both stiffness and preconditioning matrices row-by-row. Non-zero terms are stored in a real vector, while the corresponding column members are stored in an integer vector of equal length. An additional integer vector with length equal to the number of equations is used to record the start of each row inside the compact scheme (Bitoulas and Papadrakakis 1991). Thus the total storage requirements for ICPR are $N_K + N_R$ real (the size of \mathbf{K} and \mathbf{R} respectively) and $N_K + N_R + 2(n + 1)$ integer stores (for the addressing). The extra storage for the conjugate gradient method is $5n$ real positions. The direct solution procedure with the complete Cholesky factorization is handled either with two skyline storage routines for \mathbf{K} and \mathbf{L} (version a) or with a compact storage for \mathbf{K} and a skyline storage for \mathbf{L} (version b). In estimating the computer storage it is assumed that integers are stored as INTEGER *2 or INTEGER *4 according to their maximum possible values, and the floating point variables as REAL *4 or REAL *8 according to the accuracy of computation, single or double respectively.

Example 1 The first test example is the six storey space frame analysed by Orbison et al. (1982) and Conci and Gattass (1990). The frame layout and the element sections are shown in Fig. 4. The yield strength of all elements is taken 250 MPa. The beams have $L_1 = 7.32$ m and the columns $L_2 = 3.66$ m. The loads, consisting of a 19160 Pa gravity load on all floor levels and a lateral load of 109 kN applied to each node in the front elevation in the negative z direction, were proportionally applied. The number of equations is 180 and the half bandwidth is 41. In Fig. 5 the load-displacement curves are shown for the results obtained by the use of the two yield surfaces. The

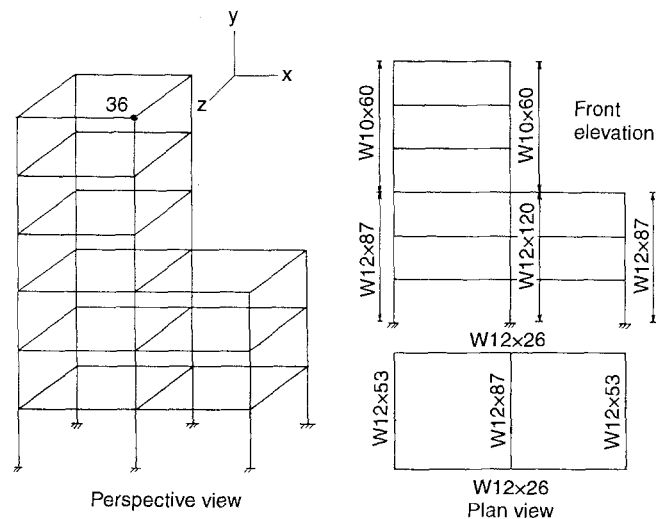


Fig. 4. Example 1-Orbison's space frame

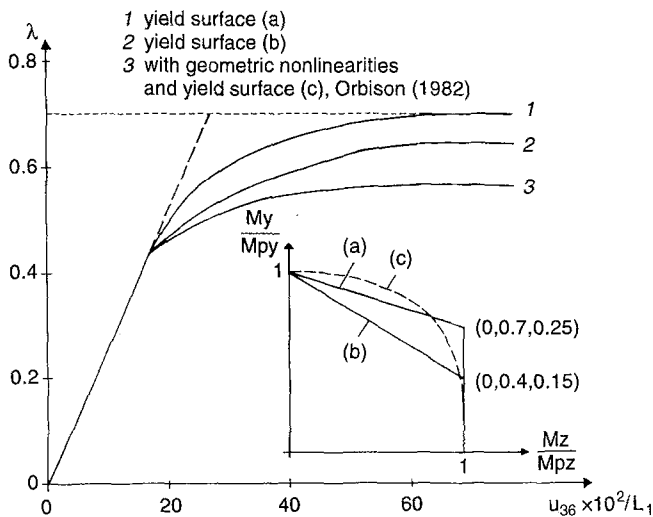


Fig. 5. Load-deflection curves of Example 1 and plan view of yield surfaces

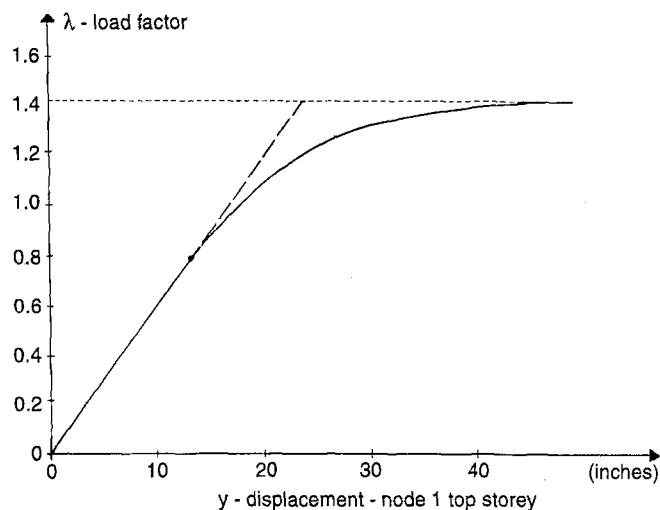


Fig. 7. Load-deflection curve of Example 2

complete Cholesky LDL^T factorization and not any PCG version is used to solve the equations at each step since this example is very small to assess the efficiency of the solution procedures described in the previous section.

Example 2 The second test example is the twenty storey space frame analysed previously by Orbison et al. (1982) and Bozzo and Gambarotta (1985), and is shown in Fig. 6 (plan (a)). The loads considered here are uniform vertical forces applied at joints and equivalent to uniform load of 100 psf and horizontal forces equivalent to uniform pressure of 20 psf on the larger surface. The load-displacement curve is shown in Fig. 7. The number of equations is 1200 and the half bandwidth is 65. Table 1 depicts the influence of the distance of the two yield

Table 1. Example 2. Accuracy and efficiency of the method for different values of the tolerance parameter ϵ_s

ϵ_s	10^{-1}	10^{-2}	10^{-4}	10^{-9}
Steps	3	65	350	350
Load factor	0.066	1.40	1.34	1.30
Number of plastic nodes	600	103	95	85
Total time(s)	7.9	99.4	502.6	504.1

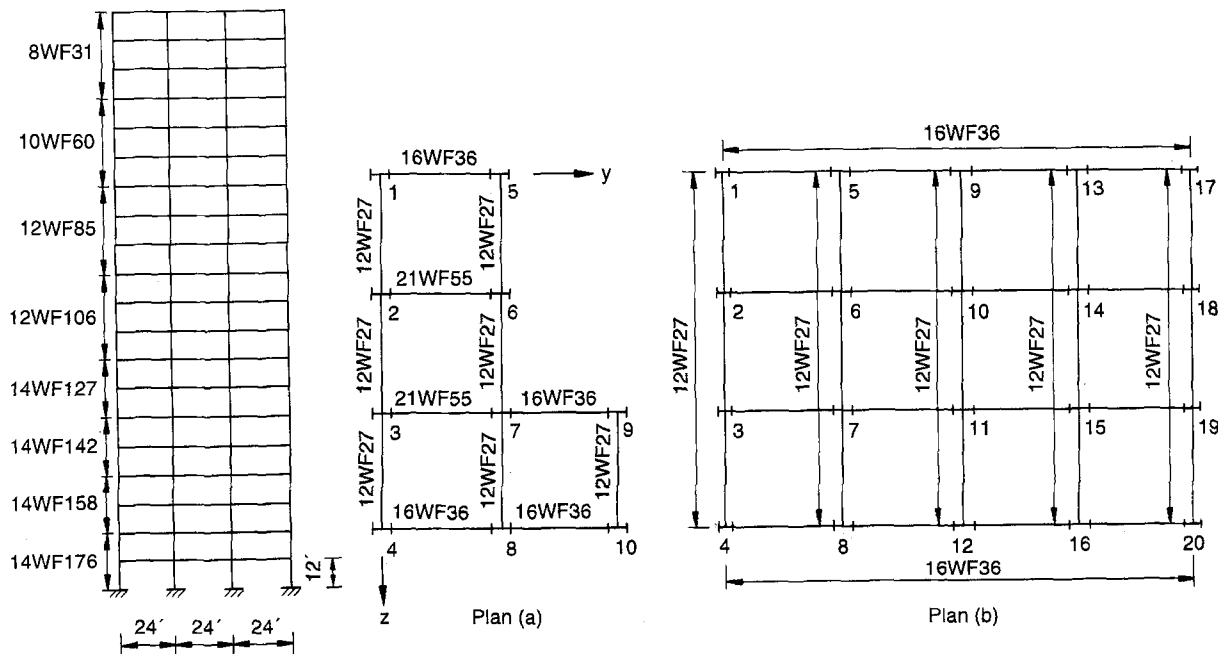


Fig. 6. Examples 2 and 3-Twenty storey space frames

surfaces, used to define the yield zone, on the accuracy and efficiency of the solution. The tolerance criterion ϵ , controls the activation of a yield mode and may be considered as being proportional to the bandwidth of the yield zone. Table 2 shows the performance of the PCG iterative solution procedure for steps 1 and 50 with the ICPR preconditioner for various values of the ψ parameter and with the SSOR preconditioner. This Table depicts the number of iterations, the CPU time, the number of elements retained during the incomplete factorization of the initial elastic stiffness and of the elasto-plastic stiffness matrix at load step 50. The time entries are in seconds as obtained by the Silicon Graphics Indigo R4000 workstation. For the subsequent applications the value of $\psi = 10^{-5}$ was selected for the ICPR preconditioner. A comparative study of the methods with the different values of the characteristic parameters appears in Table 3. The storage requirements and computing time as well as the ultimate load factor and the number of load steps as depicted for the direct method (DIR) of complete factorization with and without modification and for the PCG with ICPR ($\psi = 0$ and $\psi = 10^{-5}$) and SSOR ($\psi = 0, \omega = 1$) preconditioners. The ICPR with $\psi = 0$ corresponds to an iterative improvement proposed for the direct methods by Papadrakakis and Bitoulas (1993). The letter *M* after the abbreviated name of the method means that the modified factorization has been used. The abbreviation NUM controls the frequency of updating the preconditioning matrix. It denotes the maximum allowable ratio of PCG iterations in the current step over the iterations in the previous step before the

preconditioning matrix is updated. When updating is performed at each load step the abbreviation NUM is omitted. Finally, the mixed precision implementation of the PCG is denoted with the word 'mixed'. The factorization and substitution time is allocated to direct versions only. Two storage handlings of the stiffness matrix are contained for the

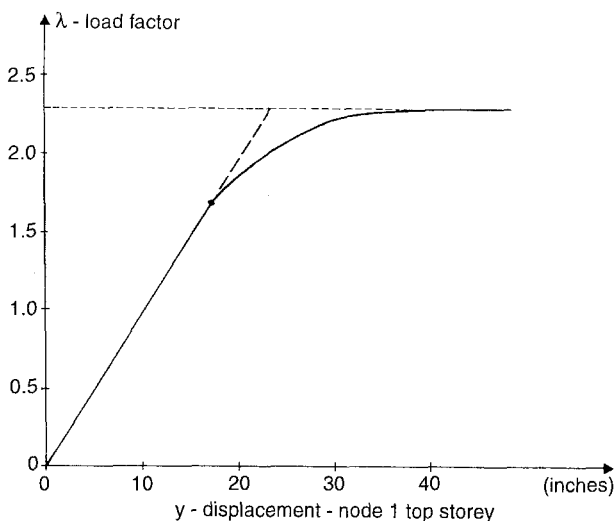


Fig. 8. Load-deflection curve of Example 3

Load step	Elements of stiffness matrix K		Elements of preconditioner R		PCG iterations		Time (s)	
	1	50	1	50	1	50	1	50
DIR	73428	73428	-	-	-	-	3.36	3.36
$\psi = 10^{-7}$	6480	7356	20078	20553	7	15	3.34	4.32
$\psi = 10^{-6}$	6480	7356	13941	14223	13	21	3.17	4.15
$\psi = 10^{-5}$	6480	7356	10027	10135	15	30	2.90	4.14
$\psi = 10^{-4}$	6480	7356	7062	7078	41	50	3.95	4.88
$\psi = 10^{-3}$	6480	7356	4653	4714	38	84	3.45	5.88
$\psi = 10^{-2}$	6480	7356	2999	3025	62	165	4.63	8.36
SSOR	6480	7356	-	-	84	208	4.78	12.17

Table 2. Example 2. Performance of ICPR for various ψ at load step 1 and 50. ($\epsilon = 10^{-1}$)

Load step	Elements of stiffness matrix K		Elements of preconditioner R		PCG iterations		Time (s)	
	1	50	1	50	1	50	1	50
DIR	284376	284376	-	-	-	-	24.10	24.10
$\psi = 10^{-7}$	16462	17126	60082	60369	11	13	11.69	11.97
$\psi = 10^{-6}$	16462	17126	38063	38192	16	19	11.05	11.56
$\psi = 10^{-5}$	16462	17126	26035	26121	22	28	10.62	11.15
$\psi = 10^{-4}$	16462	17126	17018	17035	33	40	9.83	10.40
$\psi = 10^{-3}$	16462	17126	10102	10108	43	51	9.42	10.08
$\psi = 10^{-2}$	16462	17126	9524	7528	51	61	9.15	9.70
SSOR	16462	17126	-	-	85	126	11.64	14.35

Table 3. Example 2. Efficiency of the methods for different values of the characteristic parameters

Table 4. Example 3. Performance of ICPR for various ψ at load step 1 and 50. ($\epsilon = 10^{-1}$)

METHOD	DIR	DIR-M	ICPR-M $\psi=0$ $\epsilon=10^{-1}$ NUM2	ICPR-M $\psi=0$ $\epsilon=10^{-2}$ NUM2	ICPR-M $\psi=0$ $\epsilon=10^{-2}$ NUM = 3	ICPR-M $\psi=0$ $\epsilon=10^{-2}$ NUM = 3 mixed	ICPR-M $\psi=10^{-5}$ $\epsilon=10^{-1}$ NUM2	ICPR-M $\psi=10^{-5}$ $\epsilon=10^{-2}$	ICPR-M $\psi=10^{-5}$ $\epsilon=10^{-1}$ NUM2	ICPR-M $\psi=10^{-5}$ $\epsilon=10^{-1}$ NUM3	ICPR-M $\psi=10^{-5}$ $\epsilon=10^{-1}$ mixed	SSOR $\epsilon=10^{-1}$
STORAGE (Mbytes)	1204 ^a	1204 ^a	709	709	709	329	223	223	223	223	159	118
TIME (s)	681 ^b	681 ^b	709	709	709	329	223	223	223	223	159	118
Factorization	61.2	40.1	-	-	-	-	-	-	-	-	-	-
Substitutions	4.8	4.5	-	-	-	-	-	-	-	-	-	-
Preconditioning	-	-	24.7	19.7	20.1	20.1	12.9	12.9	2.9	1.2	12.2	-
CG iterations	-	-	14.7	14.7	22.6	22.6	44.7	75.1	60.4	58.6	43.6	271.7
Plastic node	33.4	33.1	33.8	33.5	32.4	32.4	23.4	20.9	26.9	27.7	29.1	29.4
Total	99.4	77.7	73.2	67.9	75.3	75.3	81.0	108.9	90.2	87.5	84.9	301.1
Steps	65	65	58	60	60	60	50	58	50	50	55	45
Load factor	1.40	1.40	1.40	1.40	1.40	1.40	1.40	1.40	1.40	1.40	1.40	1.42
Number of plaster nodes	103	103	150	150	150	150	145	150	150	150	153	151

direct method. Case (a) corresponds to a skyline storage for both K and L , while case (b) corresponds to compact storage handling of K as used for the PCG implementations. The slack termination criterion for the linear solution is denoted by the value of ϵ .

Example 3 As a final example, an extension in plan of example 2 is chosen in order to increase the size of the problem to a more realistic structure and accentuate the capabilities and limitations of the solution techniques proposed. The plan view of the structure is shown in Fig. 6 (plan (b)). The load-displacement curve obtained is shown in Fig. 8. Table 4 depicts the performance of PCG for steps 1 and 50 and for various values of the drop-off parameter ψ . The value of $\psi = 10^{-2}$ is selected for the subsequent applications. The example was tested for selective cases obtained from example 2 and the results are shown in Table 5. In this example the incremental procedure is terminated after the 100th load increment for all cases.

5 Conclusions

The computational method presented in this work is very efficient for the first order step-by-step limit analysis of space frames. The use of the plastic node approach in conjunction with a multi-faceted approximation of the yield surface permits a linearized solution at each load step without iterations. With the implementation of a plastic zone defined by the yield surface and a second surface, homothetic and close to the first one, the efficiency of the step-by-step incremental analysis is substantially improved. Small load steps or spurious oscillations of points around the corners of the yield surface are avoided, while simultaneous formation of more than one plastic nodes at each load step is accomplished. The fact that the overall stiffness matrix changes gradually, with the successive formation of plastic nodes, enables us to implement the preconditioned conjugate gradient method for the linear solution at each load step with a complete or an incomplete Cholesky factorization of the stiffness matrix as preconditioner and to improve the efficiency of the method in both computing storage and time. Additionally, the use of a mixed precision arithmetic formulation for the preconditioned conjugate gradient method may further reduce the computer storage without impairing the computing time or the accuracy of the solution. Thus, the proposed methodology is an efficient approach for treating large realistic 3-D building frames and provides a helpful tool for the design engineer who may achieve a more optimal design by economically testing a number of design options.

More specifically, the combination of a compact storage scheme for the stiffness matrix with the modified factorization procedure, in which alterations to the factorized matrix are confined to the bottom right hand corner, appear to have a significant influence on the performance of the direct method. The storage requirements are reduced almost by half, while the computing time is less than 60% for the third example. The use of the complete factorized matrix as preconditioner for an iterative improvement of the direct method produces a 60% reduction in computing time, in respect to the modified direct method, while its mixed precision implementation results in a 50% reduction in computer storage and to a further reduction in computing time for the large example considered in this

METHOD	DIR	DIR-M	ICPR $\psi = 0$ $\varepsilon = 10^{-1}$ NUM = 2	ICPR-M $\psi = 0$ $\varepsilon = 10^{-2}$ NUM = 3	ICPR-M $\psi = 0$ $\varepsilon = 10^{-2}$ NUM = 3 mixed	ICPR-M $\psi = 10^{-2}$ $\varepsilon = 10^{-1}$	ICPR-M $\psi = 10^{-2}$ $\varepsilon = 10^{-1}$ mixed
STORAGE (Mbytes)	4607 ^a 2500 ^b	4607 ^a 2500 ^b	2555	2555	1370	375	289
TIME (s)							
Factorization	743	400	-	-	-	-	-
Substitutions	32	35	-	-	-	-	-
Preconditioning	-	-	276	98	97	80	94
CG iterations	-	-	87	111	78	216	217
Plastic node	98	98	95	95	99	90	97
Total	873	533	458	304	274	386	408
Steps	100	100	100	100	100	100	100
Load factor	2.3	2.3	2.1	2.1	2.1	2.1	2.1
Number of plastic nodes	167	167	210	210	198	205	205

Table 5. Example 3. Efficiency of the methods for different values of the characteristic parameters

study. Finally, the ICPR implementation with $\psi \neq 0$ produces competitive times in respect to the direct method with iterative improvement while requiring only 1/5 to 1/10 of the corresponding computer storage requirements of the direct method.

References

- Ajiz, M. A.; Jennings, A. 1984: A robust incomplete Cholesky conjugate gradient algorithm. *Int. J. Num. Meth. Eng.* 20: 949–966
- Al-Bermani, F. G. A.; Kitipornchai, S. 1990: Elastoplastic large deformation analysis of thin-walled structures. *J. Engineering Structures* 12: 28–36
- Argyris, J. H.; Boni, B.; Hindenlang, U.; Kleiber, M. 1982: Finite element analysis of two- and three-dimensional elasto-plastic frames. The natural approach. *Comp. Meth. Appl. Mech. Eng.* 35: 221–248
- Bathe, K. J.; Wilson, E. L. 1976: *Numerical Methods in Finite Element Analysis*. Prentice Hall Inc., Englewood Cliffs, New Jersey
- Bitoulas, N.; Papadrakakis, M. 1994: An optimised computer implementation of the incomplete Cholesky factorization, *Comp. Systems in Enging.* (to appear)
- Bozzo, E.; Gambarota, L. 1983: Inelastic analysis of steel frames for multistorey buildings. *Computer Structures* 20: 707–713
- Conci, A.; Gattass, M. 1990: Natural approach for thin walled beam columns with elastic plasticity. *Int. J. Num. Meth. Eng.* 29: 1653–1679
- Hilmy, S. I.; Abel, J. F. 1985: Material and geometric non-linear dynamic analysis of steel frames using computer graphics. *Computer Structures* 21: 825–840
- Izzudin, B. A.; Elnashai, A. S. 1993: Adaptive space frame analysis: Part I, a plastic hinge approach. *Proc. Ins. Civil. Engineers* 99: 303–316
- King, W. S.; White, D. W.; Chen, W. F. 1992: Second order inelastic analysis methods for steel-frame design. *J. Struct. Eng. ASCE* 118: 408–428
- Kondoh, K.; Atluri, S. N. 1987: Large deformation elasto-plastic analysis of frames under non-conservative loading, using explicitly derived tangent stiffnesses based on assumed stresses. *J. Computational Mechanics* 2: 1–25
- Morris, N. F. 1990: Verification of simplified inelastic models of 3-D behavior. *J. Eng. Mech. ASCE* 116: 1580–1598
- Orbison, J. G.; McGuire, W.; Abel, J. F. 1982: Yield surface applications in non-linear steel frame analysis. *Comp. Meth. Appl. Mech. Eng.* 33: 557–573
- Papadrakakis, M. 1991: Solving large-scale problems in solid and structural mechanics. M. Papadrakakis (ed.) *Solving large-Scale Problems in Mechanics*, J. Wiley, Chichester, England, pp. 1–37
- Papadrakakis, M.; Karamanos, S. A. 1991: A simple and efficient solution method for the limit elastoplastic analysis of plane frames. *J. Computational Mechanics* 8: 235–248
- Papadrakakis, M.; Bitoulas, N. 1993: Accuracy and effectiveness of preconditioned conjugate gradient method for large and ill-conditioned problems. *Comp. Meth. Appl. Mech. Eng.* 109: 219–232
- Powell, G. H.; Chen, P. F. S. 1986: 3-D beam column element with generalized plastic hinges. *J. Eng. Mech. ASCE* 112: 627–641
- Shi, G.; Atluri, S. N. 1988: Elastoplastic large deformation analysis of space frames: A plastic hinge and stress based explicit derivation of tangent stiffnesses. *Int. J. Num. Meth. Eng.* 26: 589–615
- Shi, G.; Atluri, S. N. 1989: Static and dynamic analysis of space frames with nonlinear flexible connections. *Int. J. Num. Meth. Eng.* 28: 2635–2650
- Shi, G.; Atluri, S. N. 1992: Nonlinear dynamic response of frame-type structures with hysteretic dumping at the joints. *AIAA Journal* 30: 234–240
- Tin-Loi, F.; Wong, M. B. 1989: Nonholonomic computer analysis of elastoplastic frames. *Comp. Meth. Appl. Mech. Eng.* 72: 351–364
- Ueda, Y.; Yao, T. 1982: The plastic node method: A new method of plastic analysis. *Comp. Meth. Appl. Mech. Eng.* 34: 1089–1104
- Ziemian, R. D.; McGuire, W.; Deierlein, G. G. 1991: Inelastic limit states design. Part I: Planar frame studies. *J. Struct. Eng. ASCE* 118: 2532–2568